J. Fluid Mech. (1994), *vol.* 259, *pp.* 291–303

Dynamic behaviour of a non-propagating soliton under a periodically modulated oscillation

By XUE-NONG CHEN† AND RONG-JUE WEI
Institute of Acoustics, Nanjing University, 210008, P.R. China

(Received 8 October 1991 and in revised form 28 July 1993)

It has been found theoretically and experimentally that a non-propagating soliton in a small rectangular water tank manifests dynamic behaviour when subjected to a modulated oscillation. A modification of the cubic Schrödinger equation was generalized for this case and analysed by the inverse-scattering perturbation method. The problem was reduced to a lower-dimensional one, i.e. to a pair of first-order ordinary differential equations for the amplitude and phase of the soliton, which were solved numerically. It was found that the soliton executes multi-periodic and chaotic motions under the periodically modulated oscillation. Corresponding experiments were carried out and both qualitative and quantitative agreement was obtained for the phenomena predicted and the parameter ranges in which they occur.

1. Introduction

The non-propagating soliton, i.e. a longitudinal soliton-type modulation of a parametrically and resonantly excited standing free-surface cross-wave, was first observed by Wu, Keolian & Rudnick (1984) in a small narrow rectangular water tank subjected to a simple harmonic vertical oscillation. Larraza & Putterman (1984) and Miles (1984) investigated it theoretically and both arrived at the cubic Schrödinger equation. The theory of Miles is briefly stated as follows. As the driving frequency 2ω is close to twice the natural frequency ω_1 of the lowest cross-mode, i.e. (0, 1) mode, a cross-wave of frequency ω with slowly longitudinally varying amplitude is induced. The complex amplitude of the wave satisfies a cubic Schrödinger equation modified by incorporating the weak damping and the constant parametric excitation, which admits a stable soliton solution that describes the observation of the wave by Wu *et al.* (1984). For recent review of parametrically excited waves and a progress report on the non-propagating soliton, we refer the reader to Miles & Henderson (1990), Laedke & Spatschek (1991), Guthart & Wu (1991) and Wei *et al.* (1990).

In a different context, a very interesting and enlightening review of the dynamic behaviour of waves and solitons was given by Abdullaev (1989). Mathematically integrable systems like solitons usually differ from actual physical systems where certain effects such as dissipation, parametric excitation or external forcing are unavoidable. Then the equations describing the latter may not be integrable. However, if these disturbances are small, the spatial soliton-type solutions are still expected to exist with their asymptotic states probably being no longer stationary, but dynamic, e.g. there is bifurcation or chaos. The asymptotic method of perturbation theory, in particular that based on the inverse-scattering transform, can be applied to the problem. Then the soliton solution can be carried out and the problem is reduced to

† Present address: University of Duisburg, FB7/13, 47048 Duisburg, Germany.

a finite-dimensional one in terms of characteristic soliton parameters, e.g. amplitude, phase and speed. This can be analysed more simply with existing analytical and numerical techniques. Chaotic motions of some kinds of solitons in special cases have been found theoretically.

In this paper, we consider an analogous case to Miles (1984), except that the water tank is subjected vertically to a periodically amplitude-modulated harmonic oscillation instead of a pure simple harmonic oscillation, and investigate the dynamic behaviour of the non-propagating soliton theoretically as well as experimentally. The cubic Schrödinger equation satisfied by the complex amplitude of the longitudinally modulated dominant cross-wave with weak damping and parametric excitation in Miles (1984) can be shown to hold also for the slowly time-varying parametric excitation and is generalized for this case simply by permitting the excitation to vary with time. This equation also possesses spatial soliton-type solutions, whose characteristic parameters, namely amplitude and phase, vary with time however, responding to the time-varying excitation. Employing the inverse-scattering perturbation technique (Lamb 1980) to the disturbed cubic Schrödinger equation since the damping and excitation are relatively small, we obtain a pair of first-order ordinary differential equations for the amplitude and phase of the soliton. The procedure reduces the task of investigating the infinite-dimensional problem to that of the two-dimensional one. Numerical integration of the equations is carried out with a fourth-order Runge–Kutta algorithm and solutions representing chaos and multi-periodic bifurcations are obtained in certain parameter ranges. We present the results as phase portraits and Poincaré maps. We also report results of experiments, in which the phenomena of chaotic and multi-periodic amplitude-modulated motion of the soliton were observed. The dynamic characteristics of motion of the soliton are identified from the frequency spectra of wave elevations. The theoretical model not only predicts the basic phenomena of chaos and bifurcation of the soliton qualitatively similar in nature to the experiment, but also attains quantitative agreement with respect to parameter ranges of occurrence of chaos and bifurcation when the experimentally determined damping ratio is used in the calculation.

2. Formulation

We consider in a small narrow rectangular tank of length l and breadth b filled with water to quiescent depth d, which is subjected vertically to a slowly amplitude-modulated harmonic oscillation of circular frequency 2ω, such that the vertical displacement Z is given by

$$Z = a(\tau)\cos 2\omega t, \quad a(\tau) = a_0 + a_1 \sin \Omega\tau, \tag{1}$$

where $\tau = \epsilon^2\omega t$, $\Omega = 2\pi F/\epsilon^2\omega$, F is modulation frequency and ϵ is a small parameter. A Cartesian coordinate system $Oxyz$ fixed in the tank is set with origin O located on one of sidewalls, the plane Oxy on the relatively quiet free surface, x the longitudinal direction, y the transverse and z positive upward. When half the basic driving frequency 2ω is near the natural frequency of the lowest cross-mode, a cross-wave at frequency ω with a longitudinally and slowly time-varying amplitude is induced. We extend the theories of Miles (1984) and Larraza & Putterman (1984) to describe this problem in the following. The cubic nonlinear Schrödinger equation for the complex amplitude of the dominant cross-wave is generalized as

$$\mathrm{i}u_\tau + \beta u + u_{XX} + 2|u^2|u + \mathrm{i}\alpha u + \gamma(\tau)\, u^* = 0, \tag{2}$$

where
$$X = \epsilon x/K^{\frac{1}{2}}, \quad u = (N^{\frac{1}{2}}/\sqrt{2})\,A, \tag{3}$$

$$\alpha = \frac{\bar{\delta}}{\epsilon^2}, \quad \beta = \frac{\omega^2-\omega_1^2}{2\epsilon^2\omega_1^2}, \quad \gamma(\tau) = \gamma_0(1+\gamma_1\sin\Omega\tau), \quad \gamma_0 = \frac{a_0\,\omega^2}{\epsilon^2 g}, \quad \gamma_1 = \frac{a_1}{a_0}, \tag{4}$$

$$\omega_1 = (gkT)^{\frac{1}{2}}, \quad k = \pi/b, \quad T = \tanh(kd), \tag{5}$$

$$K = \frac{1}{4k^2T}(T+kd\,\mathrm{sech}^2 kd), \quad N = \frac{k^2}{64T^4}(6T^6-5T^4+16T^2-9), \tag{6}$$

the asterisk denotes a complex conjugate, A is the amplitude of the dominant lowest cross-mode, ω_1 is the natural frequency of the mode, $\bar{\delta}$ is the damping ratio, equivalent to δ in Miles (1984), and g is the gravitational acceleration. The term γu^* is now permitted to vary slowly with time in consequence of the amplitude modulation of the driving oscillation. The linear damping ratio is here determined by matching theoretical stability analysis to experimental data as shown in the Appendix. This value is much higher than that calculated for a tank with hydrophilic walls according to Appendix C in Miles (1984). The nonlinear water surface elevation ζ in this case is then given by

$$\zeta = \epsilon\zeta_{11}\,\mathrm{e}^{-\mathrm{i}\omega t} + \epsilon^2\zeta_{22}\,\mathrm{e}^{-\mathrm{i}2\omega t} + \text{c.c.} + O(\epsilon^3), \tag{7}$$

$$\zeta_{11} = \tfrac{1}{2}A\cos ky, \quad \zeta_{22} = \tfrac{1}{2}A_2\cos 2ky, \quad A_2 = -\frac{\omega^2A^2}{8gT^4}(T^2-3). \tag{8}$$

In the absence of any amplitude modulation of the driving oscillation, i.e. where γ is constant, via the transformation

$$u \to \frac{2TN^{\frac{1}{2}}}{k}r, \quad X \to \frac{1}{2k(TK)^{\frac{1}{2}}}X, \quad N \to \frac{k^2}{8T^2}A, \quad K \to \frac{B}{4k^2T}, \tag{9}$$

equation (2) becomes identical to (4.4) in Miles (1984), which admits an asymptotically stable non-propagating soliton solution.

This disturbed cubic Schrödinger equation (2) with (7) and (8) can also be derived by another approach, namely multiple-scale perturbation method, which was used in Larraza & Putterman (1984). In order to emphasize the main points only, here we omit the details of the derivation.

As the parametric excitation varies with time, we expect the soliton still to exist, but to have dynamic behaviour. We can use the inverse-scattering perturbation technique (Lamb 1980) to analyse the problem if the terms γu^* and $\mathrm{i}\alpha u$ are small in some sense. First, we generalize the result of the evolution of the single soliton of (9.3.1), (9.4.1), (9.4.3), (9.4.12a, b) and (9.4.17a, b) in Lamb (1980). Substituting $u \to u^{-\mathrm{i}\int\lambda(\tau)\,\mathrm{d}\tau}$ into (9.3.1) in Lamb (1980), we have

$$\mathrm{i}u_\tau + \lambda(\tau)\,u + u_{XX} + 2|u^2|u = \mathrm{i}R(u), \tag{10}$$

$$u = 2\rho\,\mathrm{e}^{-\mathrm{i}\theta}\,\mathrm{sech}\,Z, \tag{11}$$

$$Z = 2\rho(X-\xi), \quad \theta = (\sigma/\rho)\,Z+\delta, \tag{12}$$

$$\sigma_\tau = -\tfrac{1}{2}\,\mathrm{Im}\int_{-\infty}^{\infty}\mathrm{d}Z(R\,\mathrm{e}^{\mathrm{i}\theta}\,\mathrm{sech}\,Z\tanh Z), \tag{13}$$

$$\rho_\tau = \tfrac{1}{2}\,\mathrm{Re}\int_{-\infty}^{\infty}\mathrm{d}Z(R\,\mathrm{e}^{\mathrm{i}\theta}\,\mathrm{sech}\,Z), \tag{14}$$

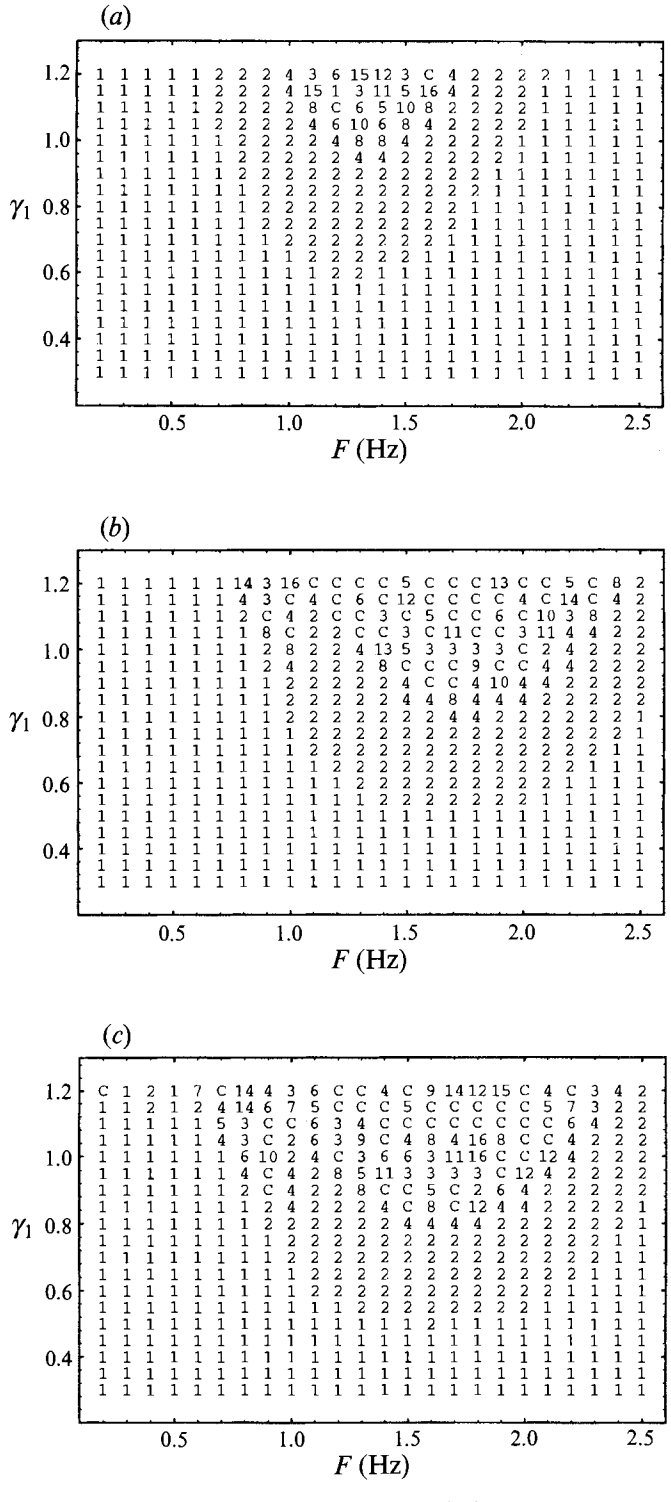

FIGURE 1(*a–c*). For caption see facing page.

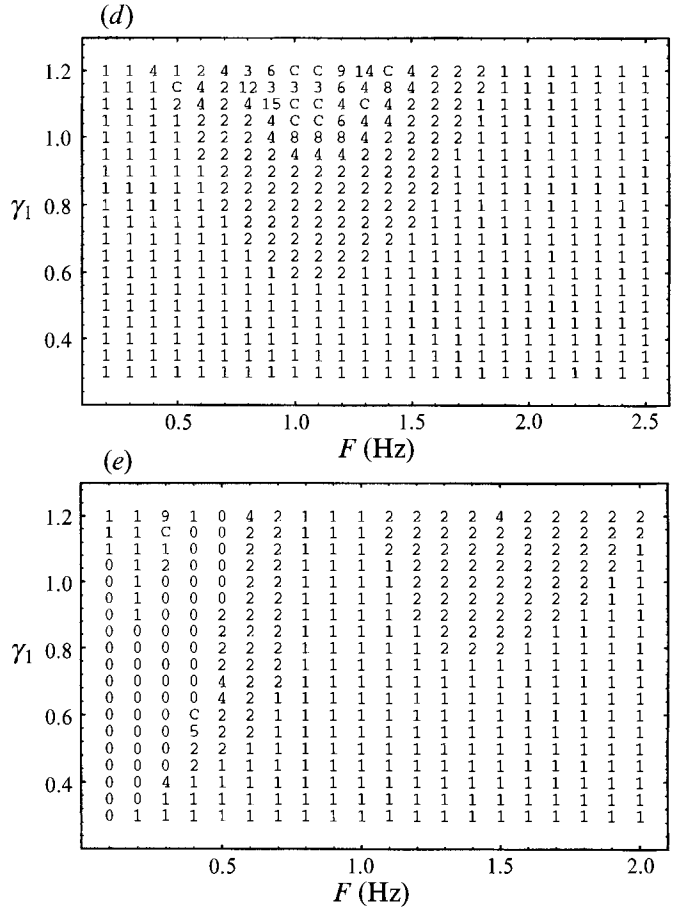

FIGURE 1. Distribution of dynamic characteristics of the soliton in the parameter plane (F, γ_1), where number denotes period multiplication and letter C means chaos; $\bar{\delta} = 0.07$ (0.068 in *e*). (*a*) $a_0 = 0.929$ mm, $2f = 10.08$ Hz; (*b*) 1.046 mm, 10.08 Hz; (*c*) 1.046 mm, 10.20 Hz; (*d*) 0.905 mm, 10.20 Hz; (*e*) 0.902 mm, 9.44 Hz.

$$\xi_\tau = -4\sigma + \frac{1}{4\rho^2}\,\mathrm{Re}\int_{-\infty}^{\infty} \mathrm{d}Z(R\,\mathrm{e}^{\mathrm{i}\theta} Z\,\mathrm{sech}\,Z), \tag{15}$$

$$\delta_\tau = -\lambda + 2\sigma\xi_\tau + 4(\sigma^2 - \rho^2) - \frac{1}{2\rho}\,\mathrm{Im}\int_{-\infty}^{\infty} \mathrm{d}Z\,R\,\mathrm{e}^{\mathrm{i}\theta}\,\mathrm{sech}\,Z(1 - Z\tanh Z), \tag{16}$$

where σ, ρ, ξ and δ are real functions of time τ, and $R(u)$ includes the small coefficient ϵ of $R(u)$ in (9.3.1) of Lamb (1980) and should be remembered as being small.

Comparing (2) with (10), we suppose (2) to have a soliton solution like (11), but the soliton is non-propagating, i.e. σ and ξ degenerate into zero and a constant, respectively, which can be proved by linear analysis if $\gamma_1 \ll 1$ and is expected still to be true even if γ_1 is not small. Thus

$$u^* = u\,\mathrm{e}^{2\mathrm{i}\delta(\tau)} \tag{17}$$

and (2) becomes (10) with

$$\lambda(\tau) = \beta + \gamma(\tau)\cos 2\delta, \quad R(u) = -[\alpha + \gamma(\tau)\sin 2\delta]\,u. \tag{18}$$

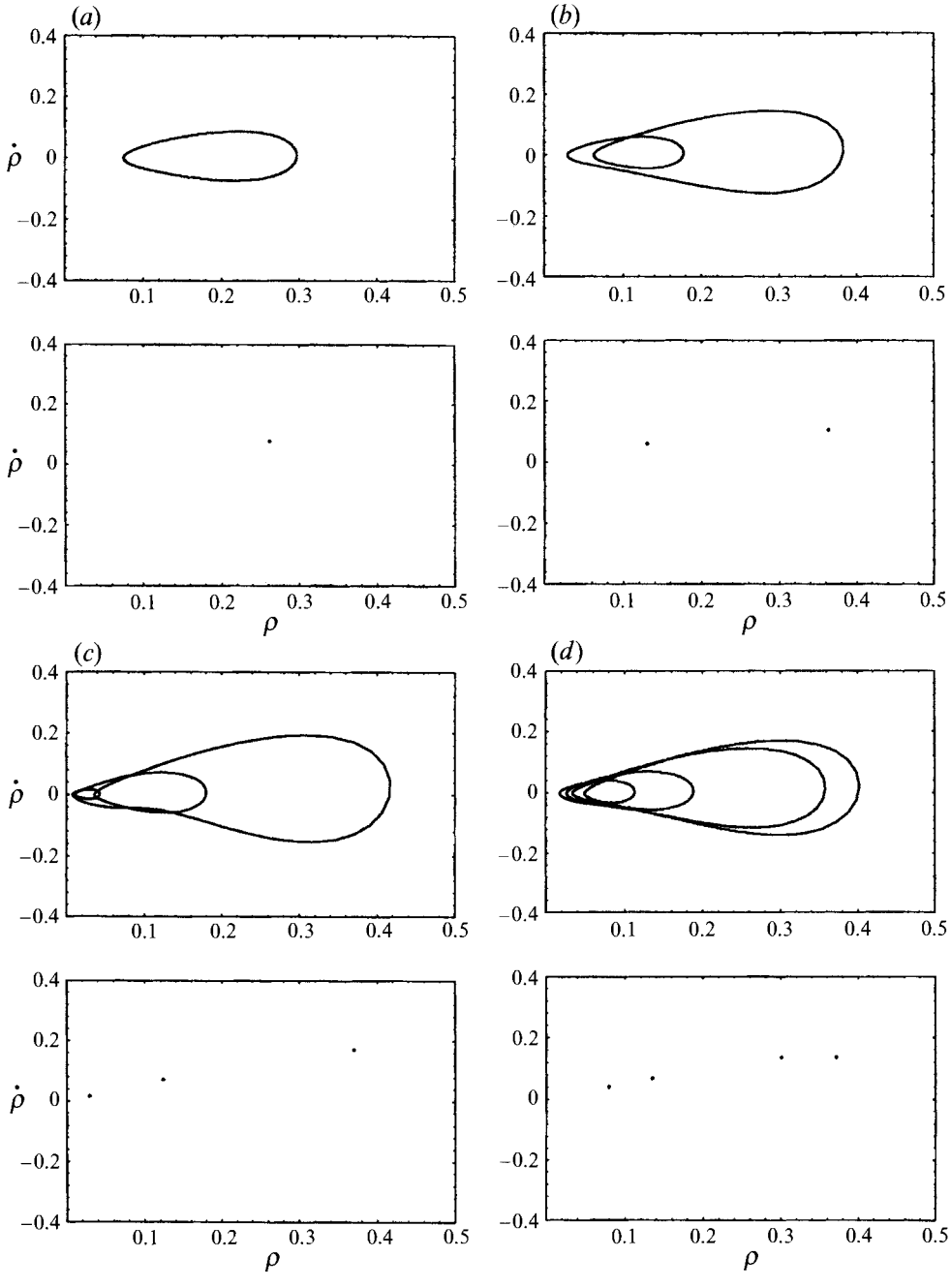

FIGURE 2(*a–d*). For caption see facing page.

Substituting (18) into (13)–(16) yields,

$$\rho_\tau = -2[\alpha + \gamma(\tau)\sin 2\delta]\rho, \tag{19}$$

$$\delta_\tau = -\beta - \gamma(\tau)\cos 2\delta - 4\rho^2, \tag{20}$$

$$\sigma = 0, \quad \xi = \xi_0 = \text{constant}. \tag{21}$$

The above equations describe a dynamic motion of the single non-propagating soliton responding to the excitation in terms of its amplitude ρ and phase δ.

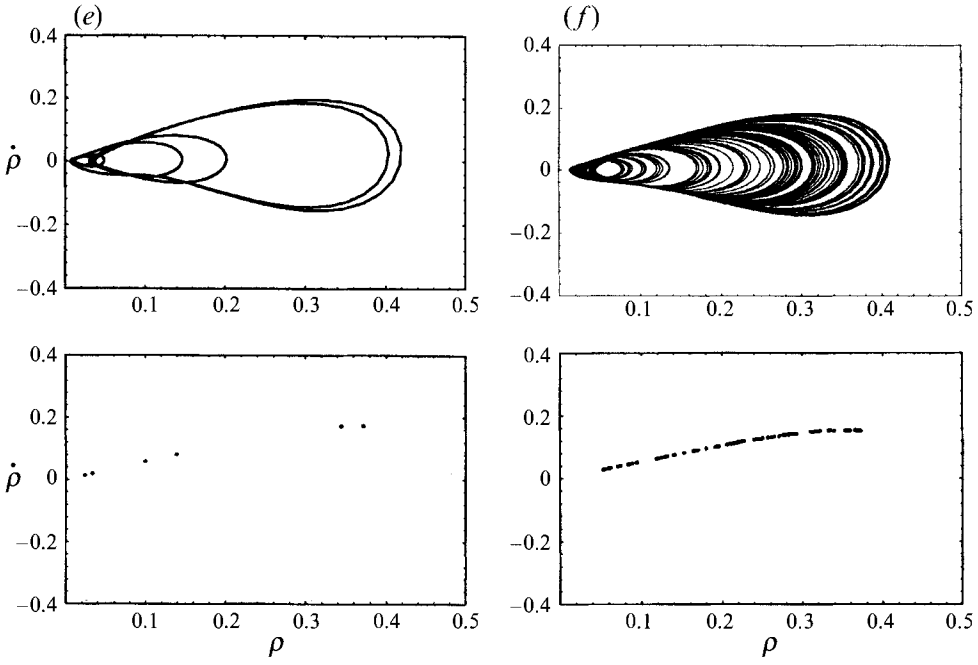

FIGURE 2. Phase portraits (top) and Poincaré maps (bottom) of some typical attractors in the phase plane $(\rho, \dot{\rho})$ for $a_0 = 0.905$ mm, $2f = 10.20$ Hz, $\bar{\delta} = 0.07$ and $F = 1.0$ Hz: (*a*) Single-period limit cycle at $\gamma_1 = 0.560$; (*b*) double-period limit cycle at $\gamma_1 = 0.800$; (*c*) triple-period limit cycle at $\gamma_1 = 1.140$; (*d*) quadruple-period limit cycle at $\gamma_1 = 0.960$; (*e*) sextuple-period limit cycle at $\gamma_1 = 1.162$; (*f*) strange attractor at $\gamma_1 = 1.050$.

If $\gamma = \gamma_0 =$ constant, a steady solution is obtained by setting $\rho_\tau = \delta_\tau = 0$ in (19) and (20),

$$\rho = \rho_0 = \tfrac{1}{2}(-\beta - \gamma_0 \cos 2\delta_0)^{\frac{1}{2}}, \tag{22}$$

$$\delta = \delta_0 = \begin{cases} \tfrac{1}{2}\pi + \tfrac{1}{2}\arcsin(\alpha/\gamma_0) & (23a) \\ -\tfrac{1}{2}\arcsin(\alpha/\gamma_0). & (23b) \end{cases}$$

A linear stability analysis based on (19) and (20) shows that only (23*a*) is stable, which is consistent with the result of (5.5) in Miles (1984).

The evolution equations (19) and (20) can also be obtained by an alternative approach, namely the Krylov–Bogoliubov integral average technique, which is called direct perturbation method by Abdullaev (1989). The single non-propagating soliton solution of (2) is assumed to be

$$u = 2\rho(\tau)\, e^{-i\delta(\tau)} \operatorname{sech} 2\rho(\tau)(X - \xi_0).$$

Substituting this expression into (2), integrating the equation with respect to X and equating the real and imaginary parts to zero, we obtain the same as (19) and (20).

Equations (19) and (20), established approximately with the perturbation method of Lamb (1980), hold when the condition of small disturbance, i.e. $|R(u)| \ll O(|u|)$, is satisfied. Here we examine it for the case $b = 3$ cm, $d = 2$ cm, $\omega = 31.4$ rad/s and $a_0 = 0.09$ cm. If we choose $\epsilon^2 = 0.3$ and $\bar{\delta} = 0.07$ (see §3), then $\gamma_0 = a_0\omega^2/\epsilon^2 g = 0.3018$ and $\alpha = \bar{\delta}/\epsilon^2 = 0.2333$. Even if $\gamma_1 = 1$, $R(u)$ expressed in (18) can be considered to be small. At the other extreme $\gamma_1 = 0$, $R(u) = 0$ for the steady soliton solution. So the method is still within its range of validity and can be applied to this problem.

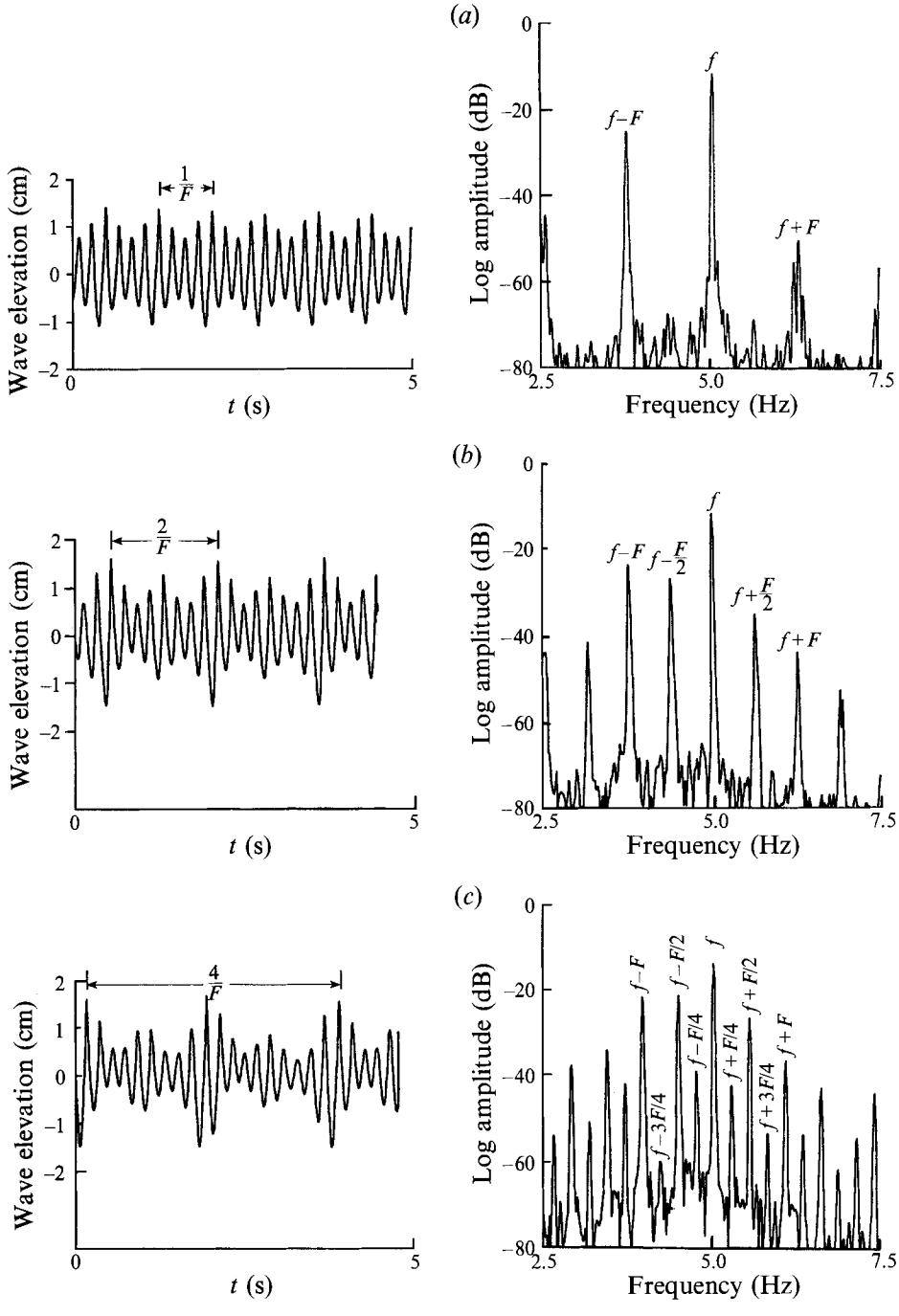

FIGURE 3(*a–c*). For caption see facing page.

3. Numerical solution

We adopt the fourth-order Runge–Kutta finite-difference algorithm to solve (19) and (20) numerically. The computer code has been checked by comparing the numerical solution with the analytical one, obtained by linearizing (19) and (20) as γ_1 is very small. All physical parameters are selected to be consistent with the anticipated

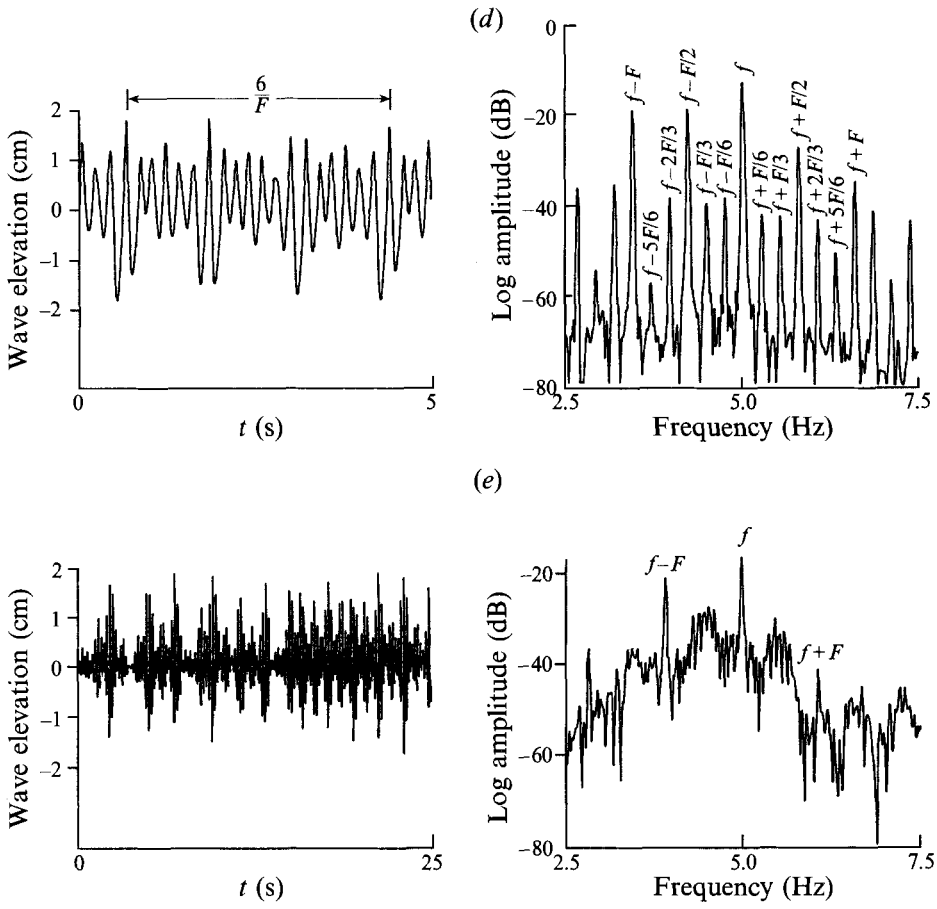

FIGURE 3. Experimental results of amplitude-modulated motions of the soliton, where the left-hand plot shows wave elevation at the centre of the soliton near either of two sidewalls and the right-hand plot shows the amplitude spectrum of the elevation; $2f = 10.20$ Hz. (*a*) Single-period motion at $a_0 = 0.925$ mm, $F = 1.30$ Hz, $\gamma_1 = 0.693$; (*b*) double-period motion at $a_0 = 0.925$ mm, $F = 1.26$ Hz, $\gamma_1 = 0.858$; (*c*) quadruple-period motion at $a_0 = 0.905$ mm, $F = 1.07$ Hz, $\gamma_1 = 0.987$; (*d*) sextuple-period motion at $a_0 = 1.06$ mm, $F = 1.62$ Hz, $\gamma_1 = 1.158$; (*e*) chaotic motion at $a_0 = 0.901$ mm, $F = 1.1$ Hz, $\gamma_1 = 1.164$.

experiment, i.e. $b = 3$ cm, $d = 2$ cm and $g = 980$ cm s^{-2}. The damping ratio $\bar{\delta}$ is set at 0.07, a value determined in the Appendix by fitting results of stability analysis to experimental data. Calculation parameters are selected suitably: $\epsilon^2 = 0.3$ and time step $\Delta\tau = 2\pi/60\Omega$. Initial values for ρ and δ are given in (22) and (23*a*) respectively, for all calculations in this paper.

The period-multiplication bifurcation and chaos in the solution of ρ and δ are found in calculations and identified by trajectories in phase plane $(\rho, \dot{\rho})$ and Poincaré maps of period $2\pi/\Omega$. The calculated dynamic characteristics of the soliton within the investigated parameter range (F, γ_1) are presented in figure 1(*a–e*), corresponding to the experimental results in table 1(*a–e*) in the next section with the same parameters, where $2f$ and F are basic and modulating frequencies, respectively. Repeated bifurcation with period doubling occurs as γ_1 increases. Also, motions of 3, 6, 5, 10 times the basic period and chaotic motion are observed as well. These typical cases of periodic motions (limit cycles or periodic attractors) presented in figure 2(*a–e*) and chaos (strange attractor) in figure 2(*f*) are shown as trajectories in phase plane $(\rho, \dot{\rho})$

and their Poincaré maps. The Poincaré maps consist of time sections at $\tau = 2\pi m/\Omega$, where m is any integer greater than 100. We can easily recognize the dynamic characteristics of the soliton motion from the figures.

4. Experiment

The experimental set-up for validating the above theory was similar to that described in Wu *et al.* (1984) or Wei *et al.* (1990). We used a small Plexiglas rectangular tank of 19.5×3 cm^2 filled with water to depth 2 cm. A little soap was added to minimize surface pinning at the walls and some cotton was placed at the two ends of the tank to eliminate other wave modes and to maintain the non-propagating solitary wave under the condition of modulated oscillation. The tank was placed on a platform that could execute a vertical periodically amplitude-modulated harmonic oscillation,

$$Z = (a_0 + a_1 \sin 2\pi Ft)\cos 4\pi ft, \quad \gamma_1 = a_1/a_0, \tag{24}$$

where γ_1 is the modulation ratio, the basic frequency $2f$ is about 10 Hz and the modulation frequency F is within 0.3–2 Hz. A pair of electrodes was inserted vertically at the centre of the soliton and near either of two sidewalls to measure the elevation of the free surface. The probe responded with a voltage between the electrodes nearly proportional to the free-surface elevation. A frequency spectrum analyser of type HP3582A was used to record the wave elevation and to obtain its spectrum.

Four parameters, a_0, f, γ_1 and F, could be controlled. Keeping $\gamma_1 = 0$ and adjusting a_0 and f in the existence range of the soliton (see the Appendix), we could generate a steady non-propagating soliton, localized in the longitudinal direction and sloshing at frequency f in the transverse direction. Choosing a suitable F within $0.3 < F < 2$ Hz and increasing γ_1 from 0 to 1.5 gradually, we observed that the soliton still existed but the amplitude of sloshing was modulated in time. When γ_1 was small, the response modulation of the wave occurred at the same period as the driving modulation $1/F$ and there were frequency peaks $f \pm mF$ in its spectrum (figure 3*a*), where $m = 0, 1, 2, \ldots$. Increasing γ_1 gradually, we found that, instead of at $1/F$, the modulation occurred at periods $2/F$, $4/F$ and $6/F$ as can be seen in the left-hand plot of figures 3(*b*), 3(*c*) and 3(*d*), respectively. Correspondingly there are peaks at $f \pm mF/2, f \pm mF/4$ and $f \pm mF/6$ in the right-hand plot of figures 3(*b*), 3(*c*) and 3(*d*), respectively, which are believed to be bifurcations of $\frac{1}{2}$, $\frac{1}{4}$ and $\frac{1}{6}$ of the amplitude modulation of the soliton. Bifurcations of further smaller fractions were not observed, possibly because their existence range was too narrow to be seen or due to the limit of resolving power of the spectrum analyser. As γ_1 exceeded a threshold, at certain values the amplitude modulation of the soliton was no longer periodic, but chaotic. The wave elevations also oscillated at the basic frequency f, but their modulation never repeated itself and there were many small peaks distributed randomly around the main peaks at f and $f \pm F$ in the spectrum (figure 3*e*). The amplitude of the wave in figure 3(*e*) stochastically approached zero and rose again, which was also found in the numerical prediction (figure 2*f*).

The dynamic behaviour of the soliton in the experiment, such as its bifurcation and chaos, identified by frequency spectra, is qualitatively consistent with the theoretical prediction. Several results for the parametric distribution of the bifurcation and chaos are given in table 1(*a–e*) that correspond to the conditions of figure 1(*a–e*), respectively. Comparison of experimental and theoretical results shows a quantitative agreement. For example, the chaos takes place at about $F = 1.1$ Hz and $\gamma_1 = 1.15$ in table 1(*a*), as it does in figure 1(*a*) also. In table 1(*e*) and figure 1(*e*) chaos occurs in similar areas; moreover when γ_1 exceeds a certain value, no soliton exists but only the

(*a*) $2f = 10.08$ Hz and $a_0 = 0.929$ mm

F (Hz)	1.00	1.12	1.32	1.60	2.00
γ_1					
0.25	1	1	1	1	1
0.40	1	1	1	1	1
0.55	1	1	1	1	1
0.70	2	2	2	2	1
0.85	2	2	2	2	2
1.00	2	C	4	2	2
1.15	C	C	C	2	2

(*b*) $2f = 10.08$ Hz and $a_0 = 1.04$ mm

F (Hz)	1.00	1.16	1.32	1.60	2.00
γ_1					
0.25	1	1	1	1	1
0.40	1	1	1	2	1
0.55	1	2	1	2	2
0.70	1	2	2	2	2
0.85	2	2	2	2	2
1.00	2	2	2	4	2
1.15	2	C	2	4	2

(*c*) $2f = 10.20$ Hz and $a_0 = 1.046$ mm

F (Hz)	1.00	1.10	1.26	1.62	2.00
γ_1					
0.25	1	1	1	1	1
0.40	1	1	1	1	1
0.55	1	1	1	2	2
0.70	1	1	2	2	2
0.85	2	2	2	2	2
1.00	2	2	2	2	2
1.15	2	C	C	6	2

(*d*) $2f = 10.20$ Hz and $a_0 = 0.905$ mm

F (Hz)	0.95	1.00	1.10	1.26	1.58	2.00
γ_1						
0.25	1	1	1	1	1	1
0.40	1	1	1	1	1	1
0.55	1	1	1	1	1	1
0.70	2	2	2	1	1	1
0.85	2	2	2	2	1	2
1.00	C	C	4	2	1	2
1.15	C	C	C	4	1	2

(*e*) $2f = 9.44$ Hz and $a_0 = 0.902$ mm

F (Hz)	0.32	0.40	0.60	0.80	1.00
γ_1					
0.25	1	1	1	1	1
0.40	1	1	1	1	1
0.55	2	1	1	1	1
0.60	C	C	1	1	1
0.70	0	C	2	1	1
0.85	0	0	2	1	1
1.00	0	0	C	1	1

TABLE 1. Experimental results for the investigated parameter range (F, γ_1), where 1, 2, 4 and 6 denote the factor by which the soliton modulation period is multiplied, C means chaotic solution, and 0 implies a relatively quiet free surface.

null solution, i.e. $\rho = 0$. We also find in both experiment and calculation that the ranges of higher fractional bifurcation, e.g. $\frac{1}{4}$ and $\frac{1}{6}$ bifurcations, are very small, even smaller than the chaotic ones.

5. Conclusion

The chaotic and multiple-periodic amplitude modulations of a non-propagating soliton subjected to a periodically modulated oscillation were found theoretically and verified experimentally. The theoretical prediction shows not only qualitative agreement with the experiment in the general appearance of the soliton, but also quantitative agreement in the parameter ranges for the occurrence of the phenomena, if the value of the damping ratio for the calculation is chosen as that determined by experiment.

We thank Professor B.-R. Wang of Nanjing University for his help in the experiments. This work was begun under the sponsorship of the Chinese National

Science Foundation and the Chinese Postdoctor Science Foundation and completed while one of the authors (X.-N.C.) was an Alexander von Humboldt Research Fellow at the University of Duisburg, Germany. We are grateful to the reviewers for their valuable suggestions and to Professor Dr.-Ing. S. D. Sharma of University of Duisburg for his help in revising the paper.

Appendix. Conditions of existence and automatic generation of the steady non-propagating soliton

It was observed by Wu *et al.* (1984) and more recently by Wei *et al.* (1990) that the single non-propagating soliton can exist stably within a certain parameter range of driving frequency and amplitude, while Miles (1984) gave a necessary theoretical condition for the existence of the soliton. In addition to these, we find that there is another threshold of driving amplitude, above which the soliton is generated automatically without any artificial initial disturbance. The following is our analysis and experimental results, which are also essential for determining the damping ratio $\bar{\delta}$ or α occurring in (4).

The evolution equations of the amplitude and phase of the soliton under the condition of unmodulated driving are contained in (19) and (20) as the special case $\gamma = \gamma_0 =$ constant. Their steady solutions are, obtained by setting $\rho_\tau = \delta_\tau = 0$, as

$$\rho_1 = \tfrac{1}{2}(-\beta - \gamma_0 \cos 2\delta_1)^{\frac{1}{2}}, \quad \delta_1 = \tfrac{1}{2}\pi + \tfrac{1}{2}\arcsin(\alpha/\gamma_0), \tag{A 1}$$

$$\rho_2 = \tfrac{1}{2}(-\beta - \gamma_0 \cos 2\delta_2)^{\frac{1}{2}}, \quad \delta_2 = -\tfrac{1}{2}\arcsin(\alpha/\gamma_0), \tag{A 2}$$

$$\rho_3 = 0, \quad \delta_3 = -\tfrac{1}{2}\arccos(-\beta/\gamma_0), \tag{A 3}$$

$$\rho_4 = 0, \quad \delta_4 = \tfrac{1}{2}\arccos(-\beta/\gamma_0). \tag{A 4}$$

We now do a stability analysis of these conditions. Suppose

$$\Delta\rho_i = \rho - \rho_i, \quad \Delta\delta_i = \delta - \delta_i, \tag{A 5}$$

which on substitution into (19) and (20) yields

$$\frac{\mathrm{d}}{\mathrm{d}\tau}\begin{pmatrix}\Delta\rho_i \\ \Delta\delta_i\end{pmatrix} = \begin{pmatrix}-2(\alpha+\gamma_0 \sin 2\delta_i) & -4\gamma_0\rho_i \cos 2\delta_i \\ -8\rho_i & 2\gamma_0 \sin 2\delta_i\end{pmatrix}\begin{pmatrix}\Delta\rho_i \\ \Delta\delta_i\end{pmatrix}. \tag{A 6}$$

The two eigenvalues of above equations are

$$\lambda_{1,2} = -\alpha \pm (\alpha^2 - C)^{\frac{1}{2}}, \tag{A 7}$$

where

$$C = -4\gamma_0 \sin 2\delta_i(\alpha + \gamma_0 \sin 2\delta_i) - 32\rho^2\gamma_0 \cos 2\delta_i. \tag{A 8}$$

According to the linear analysis theory, the solutions in (A 1)–(A 4) are stable only if both $\mathrm{Re}\,\lambda_1 \leqslant 0$ and $\mathrm{Re}\,\lambda_2 \leqslant 0$. Calculating (A 6) for each solution in (A 1)–(A 4) yields that (ρ_2, δ_2) and (ρ_4, δ_4) are always unstable, (ρ_1, δ_1) is stable if

$$\gamma_0 \geqslant \alpha > 0 \quad \text{and} \quad -\beta + (\gamma_0^2 - \alpha^2)^{\frac{1}{2}} \geqslant 0 \tag{A 9}$$

and (ρ_3, δ_3) is stable if $\quad \gamma_0^2 \geqslant \beta^2 \quad$ and $\quad \alpha - (\gamma_0^2 - \beta^2)^{\frac{1}{2}} \geqslant 0.$ (A 10)

The stability condition (A 9) is the necessary condition for existence of the soliton. It is the same as (5.7*a*, *b*) of Miles (1984). The stability condition (A 10) is the necessary condition for the free surface to remain quiescent. Hence, if

$$\gamma_0^2 > \alpha^2 + \beta^2, \tag{A 11}$$

then the condition (A 10) is broken, so the free surface cannot remain still. At the same

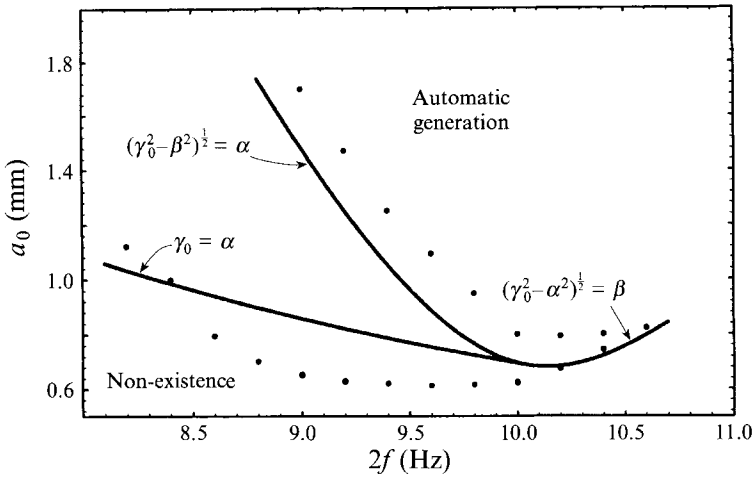

FIGURE 4. Experimental and theoretical conditions for the existence and automatic generation of the steady non-propagating soliton, where lower and upper dots denote the experimental existence and automatic generation conditions, respectively, while lower and upper solid lines denote the theoretical ones, respectively, for $\bar{\delta} = 0.07$.

time, the soliton existence condition (A 9) is satisfied, so a soliton is generated automatically under the condition (A 11).

Measurements at these two conditions of stable existence and automatic generation of the soliton were included in our experiments. The results are presented as dots in figure 4. Comparing with the theoretical conditions (A 9) and (A 11) for $\bar{\delta} = 0.07$, shown as lines in figure 4, we find that the analytical results agree well with the measured ones. This also means that the value of $\bar{\delta}$ can be estimated by matching the theoretical curves to the experimental data. Here, this gives $\bar{\delta} = 0.07$.

Conventionally, it is expected that the soliton would exist in a closed domain in the parameter plane $(a_0, 2f)$. So an upper limit for the existence of the soliton could also be expected to exist. But from the experiment, it was not as clear as the lower limit and theoretical analysis does not yield any upper limit at all. Therefore, it has not been drawn in figure 4.

REFERENCES

ABDULLAEV, F. KH. 1989 Dynamical chaos of solitons and nonlinear periodic waves. *Phys. Rep.* **179**, 1–78.

GUTHART, G. S. & WU, T. Y.-T. 1991 Observation of a standing kink cross wave parametrically excited. *Proc. R. Soc. Lond.* A **434**, 435–440.

LAEDKE, E. W. & SPATSCHEK, K. H. 1991 On localized solutions in nonlinear Faraday resonance. *J. Fluid Mech.* **223**, 589–601.

LAMB, G. L. 1980 *Elements of Soliton Theory*. John Wiley & Sons.

LARRAZA, A. & PUTTERMAN, S. 1984 Theory of non-propagating surface-wave solitons. *J. Fluid Mech.* **148**, 443–449.

MEI, C. C. 1983 *The Applied Dynamics of Ocean Surface Waves*. Wiley-Interscience.

MILES, J. W. 1984 Parametrically excited solitary waves. *J. Fluid Mech.* **148**, 451–460.

MILES, J. W. & HENDERSON, D. 1990 Parametrically forced surface waves. *Ann. Rev. Fluid Mech.* **22**, 143–165.

WEI, R., WANG, B., MAO, Y., ZHENG, X. & MIAO, G. 1990 Further investigation of nonpropagating solitons and their transition to chaos. *J. Acoust. Soc. Am.* **88**, 469–472.

WU, J., KEOLIAN, R. & RUDNICK, I. 1984 Observation of non-propagating hydrodynamic soliton. *Phys. Rev. Lett.* **52**, 1421–1424.